

CHAPTER 5

INTER-SCALE THRESHOLD BASED WAVELET FILTER (ISTWF)

5.1 INTRODUCTION

The basic principle underlying wavelet based denoising is that the wavelet coefficients of a noise corrupted image are separated into original signal coefficients and the rest as noise coefficients based on a threshold. The two groups of coefficients are then subjected to thresholding through certain rules. In most of the existing methods, the coefficients grouped as noise are made zero, resulting in an impulsive behaviour at the output.

The impulsive nature of soft thresholding as discussed in Andria et al (2013) is shown in Figure 5.1. Speckle noise is commonly observed as a granular structure that produces low magnitude wavelet coefficients. By applying proper thresholding rule, these low magnitude coefficients can be removed. This formulation is based on the empirical observation that the wavelet details in the sub-bands of a high quality US image exhibit a heavy tailed distribution, whereas a noisy image provides wavelet coefficients generally characterized by a smoothed distribution as discussed by Andria et al (2013) is shown in Figure 5.1. Figure 5.1(g) to 5.1(i) show histogram of the output of soft thresholding. It shows an impulsive distribution. This high impulsive behavior of the soft thresholding operator is a result of killing of too many coefficients including the significant coefficients. This is due to the large value of the threshold that sets too many coefficients to zero.



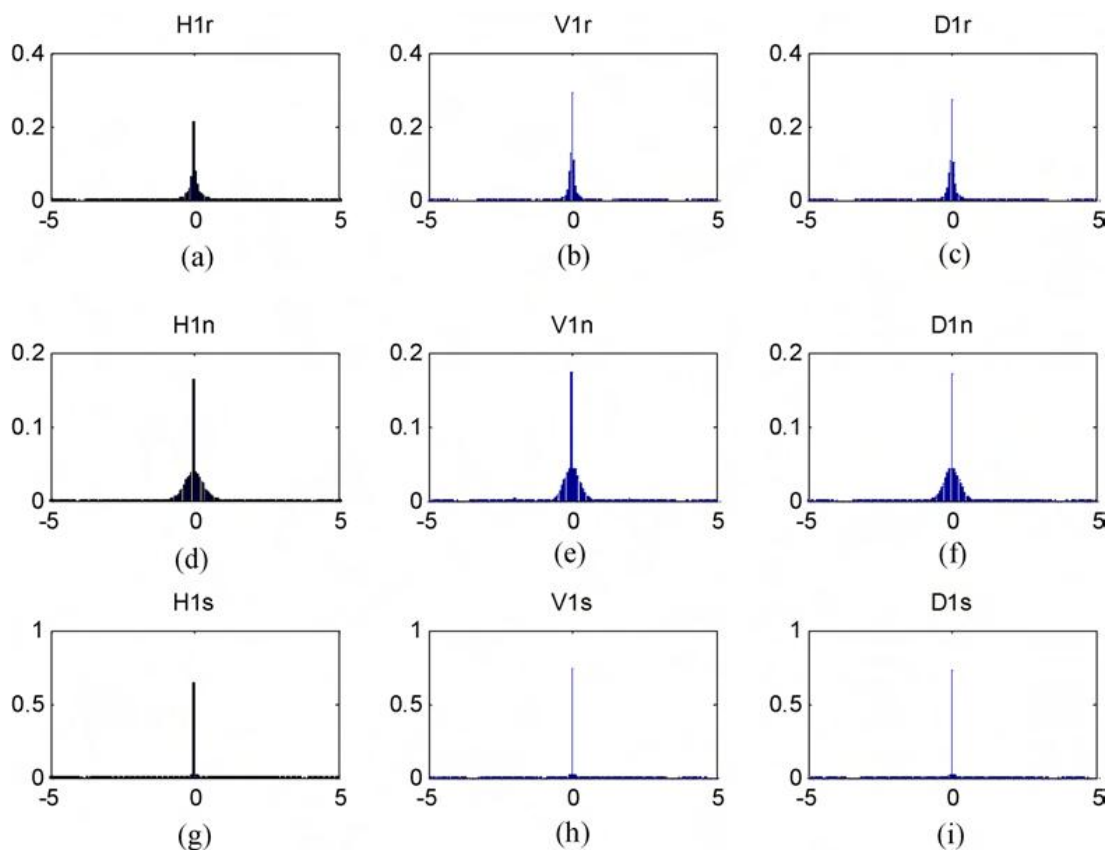


Figure 5.1 Histogram of original coefficients (a-c), noisy coefficients (d-f) and soft thresholded coefficients (g-i)

Thresholding operation, builds a zone around zero, in which the coefficients are considered negligible. The aim of this chapter is to provide a new thresholding function that can gradually reduce the coefficients in the zero zone. The objective of this function is to offer a more effective filtering scheme with improved edge preservation, by modifying the coefficients below the threshold. Also it contributes a new adaptive threshold determination technique exploiting the parent-child relationship of the pixels in the adjacent levels.

5.2 INTER-SCALE THRESHOLD BASED WAVELET FILTER (ISTWF)

Figure 5.2 shows the block diagram of the ISTWF approach. An undecimated wavelet transform is applied to decompose the input image into

l levels $\{l = 1, 2, \dots, L\}$. Each level consists of one approximation (LL) and three details subbands (LH, HL, HH) of the same size as that of the original image. The parameters required for threshold determination are estimated from the details subbands and the adaptive threshold is determined. A new exponential threshold function is proposed for modifying the coefficients below threshold. All the details coefficients are subjected to thresholding with this exponential thresholding function and the denoised coefficients are reconstructed using inverse wavelet transform.

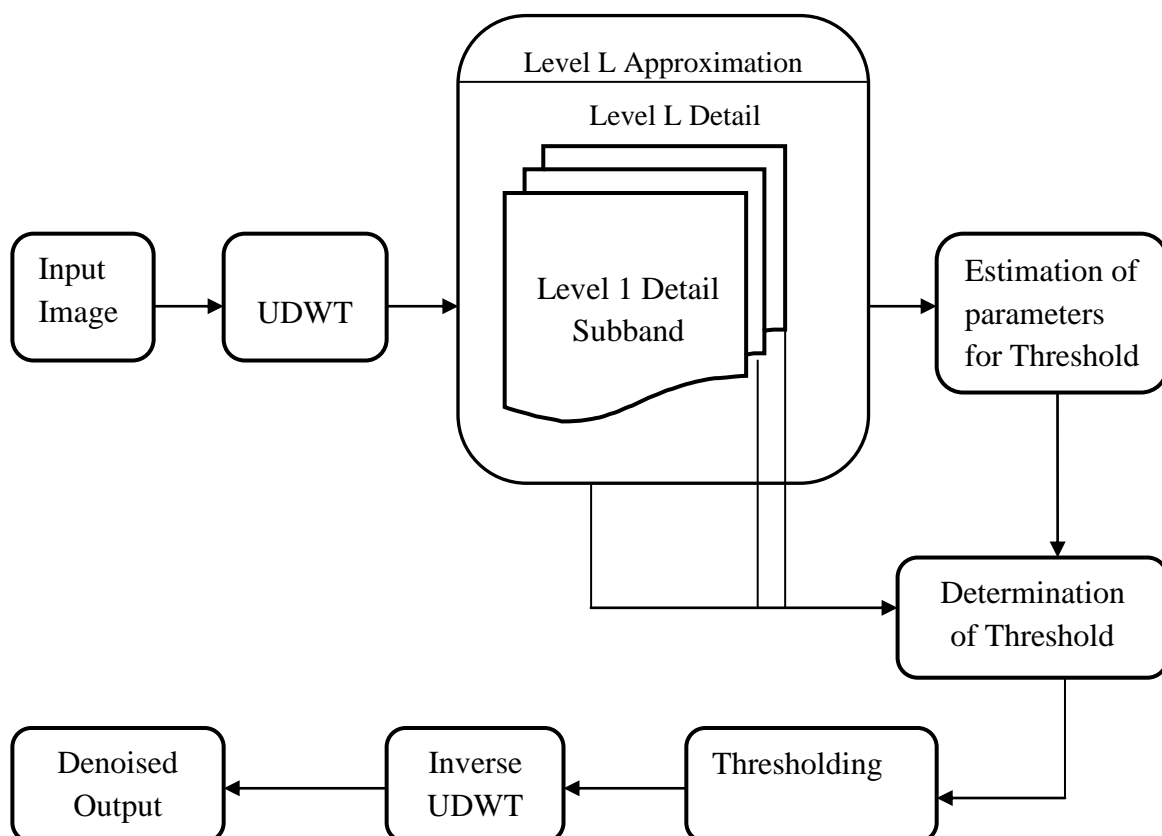


Figure 5.2 Block Diagram of ISTWF

5.2.1 Background

The functionality of noise removal filters is such that it passes all the image data present in coarser scale. The image data present in the fine scale is allowed to pass through the filter, if it is around an identified edge, otherwise it

is removed as noise. For the reason that most noise power is restricted to small resolution scales, the eradication of signal at these small scales suppress noise to a large extent. However, the information from small scale signals are required to keep the edges sharp, (Xu et al 1994). Puvanathan and Bizheva (2007) studied that large image features are established in many scales of the wavelet decomposition, whereas small image features are found only in fine resolution scales. By utilizing inter-scale correlation relating to two adjacent scales, such smaller image features at finer wavelet decomposition levels can be retained better.

The key issue in this regard is the identification of significant features of interest (edges) at smaller resolution scales. Edges in wavelet analysis are features which have signal peaks across several scales. This is based on the fact that edges coincide with large magnitude coefficients, a property of wavelet transform. Now, by analyzing the spatial correlation of the subband coefficients at different resolution scales, the features of interest can be identified. The finest scale data are retained at positions where there is a large spatial correlation and is not allowed by the filter, where there is a minimum correlation. Hence, the efficiency of retaining the small scale image data could be better evolved, through the analysis of inter-scale correlations. The inter-scale correlation based spatial adaptive threshold proposed in this chapter keeps the low magnitude coefficients which are identified around an edge. This improves the feature preserving ability of the filter.

5.2.2 Inter-scale Adaptive Threshold Determination

Selection of threshold is a crucial part in any wavelet denoising algorithm. This is due to the fact that it separates the unwanted coefficients contributing to noise and the significant signal coefficients required to reconstruct the image. It cannot be selected to be too high nor too low. A too high threshold suppresses noise to a good extent but fails to retain the



important image details. On the other hand, a too small threshold preserves the image features, but the noise is not sufficiently reduced. Hence an optimum threshold is to be selected. Most of the thresholds introduced in the literature are uniform or subband adaptive. Spatial adaptive threshold determined using context based approaches as in several literatures involve complex computations. This chapter introduces a simple and efficient method of threshold determination exploiting the dependencies of the wavelet coefficients present in adjacent scales.

Shrinking of wavelet coefficients with constant threshold kills all the low magnitude coefficients below the threshold. Therefore, the processing of the coefficients below the threshold could be well treated with an adaptive threshold varying with respect to the spatial characteristics of the pixels. The spatial adaptive threshold proposed in this chapter is determined by scaling the subband adaptive Bayesian threshold using the parent-child relationship of the adjacent scale coefficients. First the threshold for each subband is calculated using the formula $\lambda_{MB} = \rho * T_B$ as in section (3.2.3), where T_B is the Bayes threshold and ρ is the subband adaptation parameter. The procedure for determining the proposed adaptive threshold is discussed in the following section.

For a coefficient $W^l(i, j)$ in a subband, its parent coefficient is $W^{l+1}(i, j)$. If the magnitude of a coefficient in the parent subband is relatively high, then the corresponding child coefficient's magnitude will also be high. If a coefficient in the parent subband is zero then the corresponding child coefficient will also be zero or low. Using this concept, the proposed adaptive threshold is calculated. The inter-scale based adaptive threshold $T_{IS}(i, j)$ is calculated as in Equation (5.1).



$$T_{IS}(i, j) = \frac{\lambda_{MB}}{1 + K * \frac{|W^{l+1}(i, j)|}{\max |W^l(i, j)|}} \quad (5.1)$$

where λ_{MB} the subband adaptive threshold and $W^{l+1}(i, j)$ is the denoised parent coefficient and $W^l(i, j)$ is the child coefficient. The parameter K is used to adjust the scaling and it is determined experimentally to be equal to 4. The threshold T_{IS} is formulated to achieve the following adaptations in the threshold λ_{MB} . If the parent coefficient is low, then the threshold is made higher to strongly suppress the current coefficient, as the original coefficient is likely to be low. On the other hand, if the parent coefficient is high, then the threshold is made lower to keep the current coefficient as it represents a signal. This procedure is carried out for all the subbands to find the threshold for each coefficient.

5.2.3 Proposed Exponential Thresholding Function

The ability of the shrinkage functionality is dependent on both the selection of threshold and thresholding rule. The thresholding function defined in this section aims to reduce the number of zero coefficients (low magnitude coefficients). It reduces the coefficients around the zero zone gradually to zero. It is defined as,

$$\hat{W}(i, j) = \begin{cases} W(i, j) \exp(|W(i, j)| - T_{IS}(i, j)) & \text{for } |W(i, j)| < T_{IS}(i, j) \\ W(i, j) & \text{for } |W(i, j)| \geq T_{IS}(i, j) \end{cases} \quad (5.2)$$

where $\hat{W}(i, j)$ is the denoised output and $W(i, j)$ is the original coefficient.

Figure 5.3 shows the comparison of proposed thresholding function with Soft thresholding and Andria et al (2013). The parametric thresholding



approach discussed by Andria et al (2013) modified the coefficients below threshold. Their approach was dependent on two parameters that are to be determined experimentally.

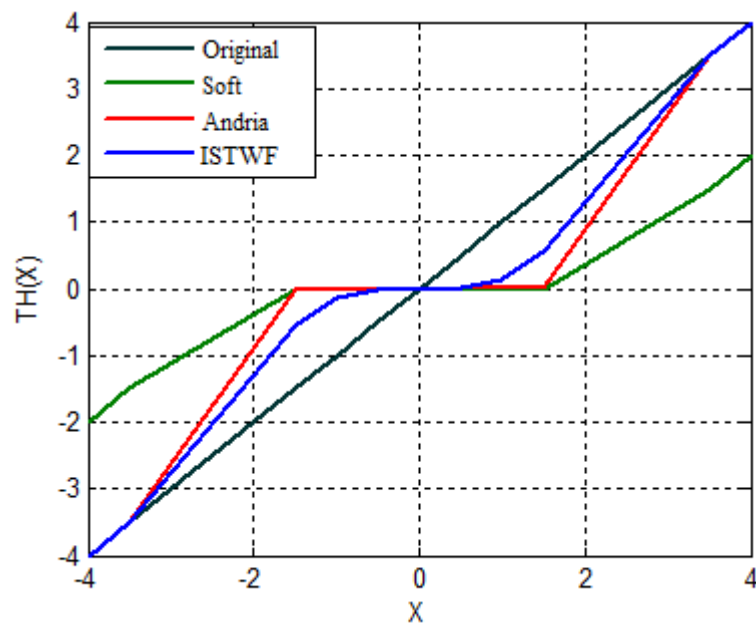


Figure 5.3 Comparison of thresholding function of ISTWF with soft thresholding and Andria et al approaches

Figure 5.3 clearly illustrates that the zero coefficients of ISTWF are gradually reduced to zero better than Andria et al (2013) approach. Also the reconstructed coefficients approach closer to the original values than Andria et al (2013). This is achieved by means of the threshold that exploits the parent child relationship among the coefficients in the adjacent scales. Figure 5.4 shows the plot of original and the reconstructed coefficients with Bayes and inter-scale threshold near the threshold zone for vertical subband at level2. It is seen that the reconstructed coefficients are set to zero after thresholding with Bayes threshold. But in inter-scale thresholding, the reconstructed coefficients are mostly approaching their original value, with individual thresholds for each of them.

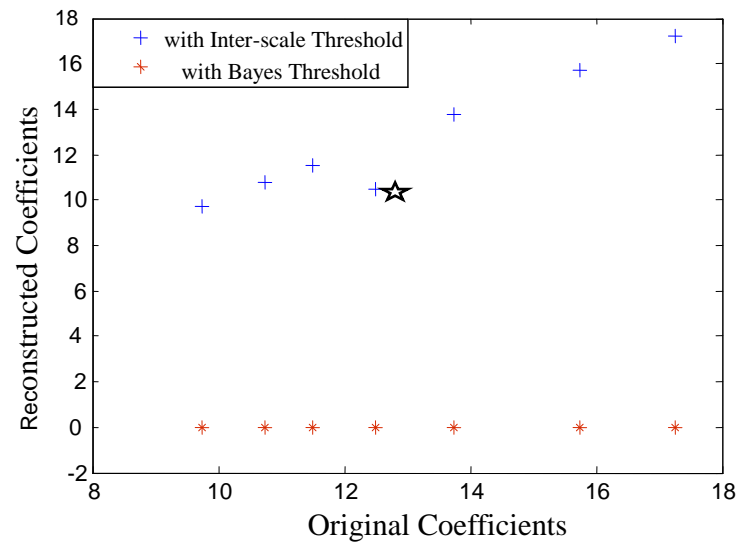


Figure 5.4 Original and reconstructed coefficients using Bayes and inter-scale threshold values

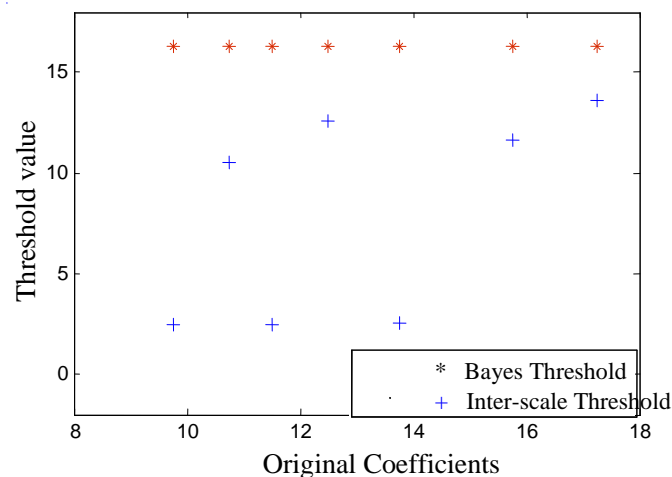


Figure 5.5 Comparison of Bayes and inter-scale threshold values

The pixel shown with star mark in Figure 5.4 has a high value at level2 and it takes up a low magnitude at level1. As per wavelet theory, if a coefficient is large at coarser scale, it is a significant pixel. Hence it is to be retained during thresholding, not to be made zero. When subjected to thresholding using bayes threshold it was reconstructed as zero as its value is less than the threshold. But the proposed threshold reconstructed the coefficient with smaller magnitude and not zero. This is how all the significant pixels are



retained based on the persistence of the wavelet coefficients across scales with the calculated robust adaptive threshold. Figure 5.5 shows the comparison of threshold values for Bayes and the interscale methods. It is evident from the figure that bayes threshold (*) is uniform for all the coefficients. The interscale threshold (+) is adaptive depending upon the coefficient values and the threshold selection is adaptive for each pixel location.

5.2.4 Summary of the Denoising Algorithm for ISTWF

The algorithm for proposed Inter Scale Threshold based Wavelet Filter (ISTWF) is summarized as follows:

Step 1: Compute the forward stationary wavelet transform of the input image to L resolution levels

Step 2: For each scale of decomposition 2^l , $l= 1 \dots L-1$

- For each detail subbands (HL,LH and HH),
 - Determine λ_{MB} using Equations (3.13) to (3.15)
 - Calculate the threshold T_{IS} using Equation (5.1)
 - Apply thresholding using the exponential thresholding function as in Equation (5.2)

Step 3: Take inverse stationary wavelet transform

5.3 RESULTS AND DISCUSSION

The performance of ISTWF is verified with simulated phantom image as well as with clinical ultrasound images. The comparisons of a simulated phantom image for various filters are shown in Figure 5.6.



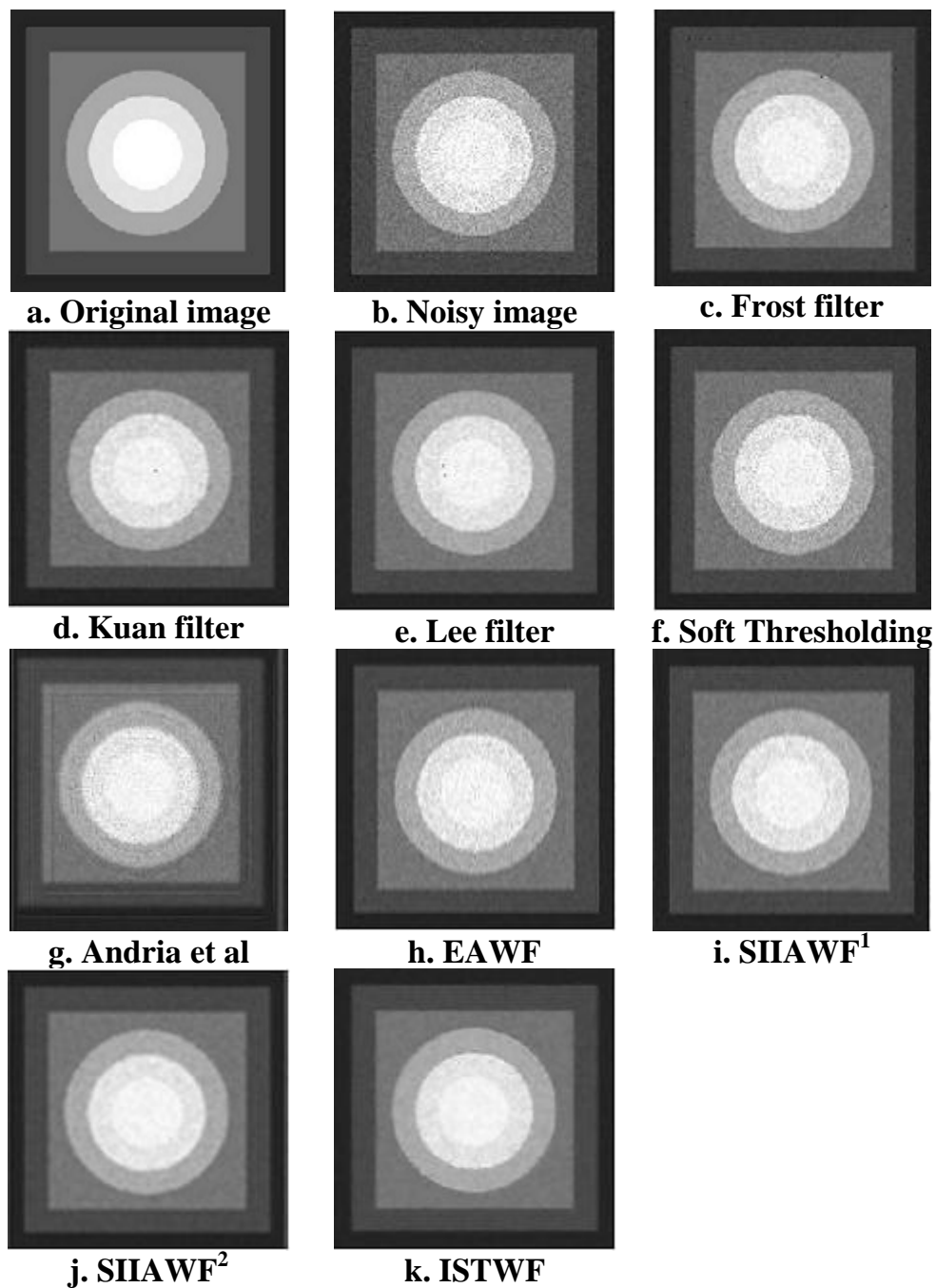


Figure 5.6 Comparison of visual quality of ISTWF with existing filters for synthetic phantom image

The results in Figure 5.6 show that ISTWF presents an enhanced quality image than the rest of the filters compared. The edges are sharper in the reconstructed output and the contrast is also improved. The performance analyses of ISTWF for various clinical US images are discussed below. Three US images in Figure 3.6 to Figure 3.8 are used as input images. The

performance of the filter simulated with different noise variances for US image1 is presented in Table 5.1.

Table 5.1 Performance comparison of ISTWF for different noise variances and filters

σ^2	Noisy	Frost	Kuan	Lee	Soft	Andria	ISTWF
	Peak Signal to Noise Ratio						
0.01	34.9435	38.6438	39.8387	39.7923	36.2507	37.7669	41.8049
0.04	31.4191	34.0636	35.5479	35.5193	33.1247	36.4700	37.7267
0.08	30.4078	31.8946	32.9930	32.8841	32.0909	35.4882	36.6229
0.1	30.1131	31.2677	32.0888	32.0758	31.7935	35.1771	35.8921
	Mean Square Error						
0.01	20.8321	8.8859	6.7485	6.8211	15.4175	10.8379	4.2913
0.04	46.8998	25.5104	18.1254	18.2455	31.6673	14.6588	10.9752
0.08	59.1965	42.0362	32.6425	33.4712	40.1782	18.3705	14.1512
0.1	63.3536	48.5639	40.1979	40.3180	43.0259	19.7411	16.7443
	Structural Similarity Index Measure						
0.01	0.9663	0.9804	0.9819	0.9820	0.9666	0.9566	0.9840
0.04	0.8882	0.9451	0.9512	0.9515	0.9135	0.9148	0.9496
0.08	0.8104	0.9023	0.9145	0.9124	0.8559	0.8886	0.9347
0.1	0.7815	0.8798	0.8944	0.8938	0.8311	0.8692	0.9052
	Equivalent Number of Looks						
0.01	1.6661	1.7021	1.6975	1.6994	1.6419	1.6796	1.7281
0.04	1.5483	1.6716	1.6844	1.6848	1.5643	1.6761	1.7693
0.08	1.4127	1.6304	1.6648	1.6636	1.4767	1.6718	1.7660
0.1	1.3606	1.6065	1.6564	1.6593	1.4347	1.6699	1.7451
	Edge Preservation Index						
0.01	0.3274	0.2622	0.2244	0.2213	0.3486	0.5848	0.7048
0.04	0.1722	0.1552	0.1646	0.1628	0.1759	0.4527	0.5791
0.08	0.1239	0.1085	0.1312	0.1262	0.1221	0.4021	0.5469
0.1	0.1114	0.0974	0.1100	0.1121	0.1072	0.3892	0.5277

Table 5.1 exhibits the comparison of various performance measures of ISTWF and some existing spatial domain and wavelet domain filters. The results in Table 5.1 are generated with haar wavelet function. Haar wavelet is selected based on the comparison of various wavelet functions given in Table 5.2.



Table 5.2 Comparison of performance metrics of ISTWF for different wavelets

Wavelets Metrics	db4	Coif2	Sym2	bior1.1	haar
PSNR	39.8551	40.5756	40.8551	39.1370	41.5452
MSE	8.0214	6.5240	6.2420	7.9320	4.5557
SSIM	0.9291	0.9637	0.9662	0.9289	0.9639
ENL	1.7068	1.7095	1.7121	1.7071	1.7556
EPI	0.6332	0.7295	0.7349	0.6329	0.7380

From Table 5.2 it is seen that PSNR, ENL and EPI values are high for haar wavelet with reduction in MSE. SSIM value is also significantly good. Hence haar wavelet is selected. The performance of ISTWF is compared with spatial domain speckle filters, soft thresholding approach and Andria et al (2013) approach. The results of comparison reveal the improved performance of ISTWF compared to other filters. PSNR is increased on an average by 4.70dB compared to soft thresholding and 1.79dB compared to Andria et al (2013) for US image1. MSE has been reduced on an average of 65.84% than soft thresholding and 30.92% than Andria et al (2013) for US image1. EPI for the proposed approach is increased on an average of 69.38% compared to soft thresholding and 22.89% than Andria et al (2013) for US image 1. SSIM measure is increased for all the noise variances and all the values are nearing the maximum value. Hence it keeps the structural information intact, in the reconstructed image.



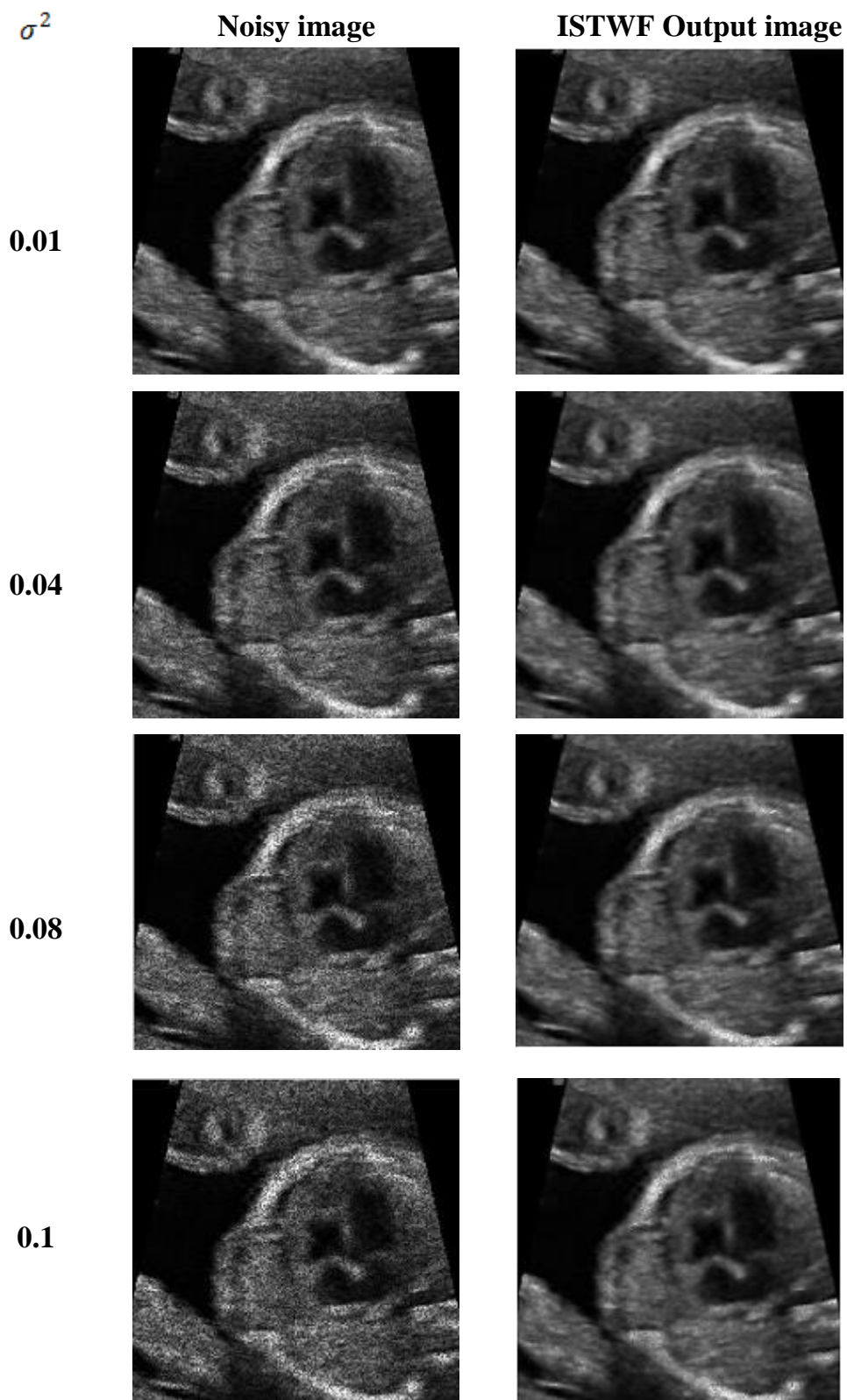


Figure 5.7 Comparison of visual quality of ISTWF for different noise variances for US image1

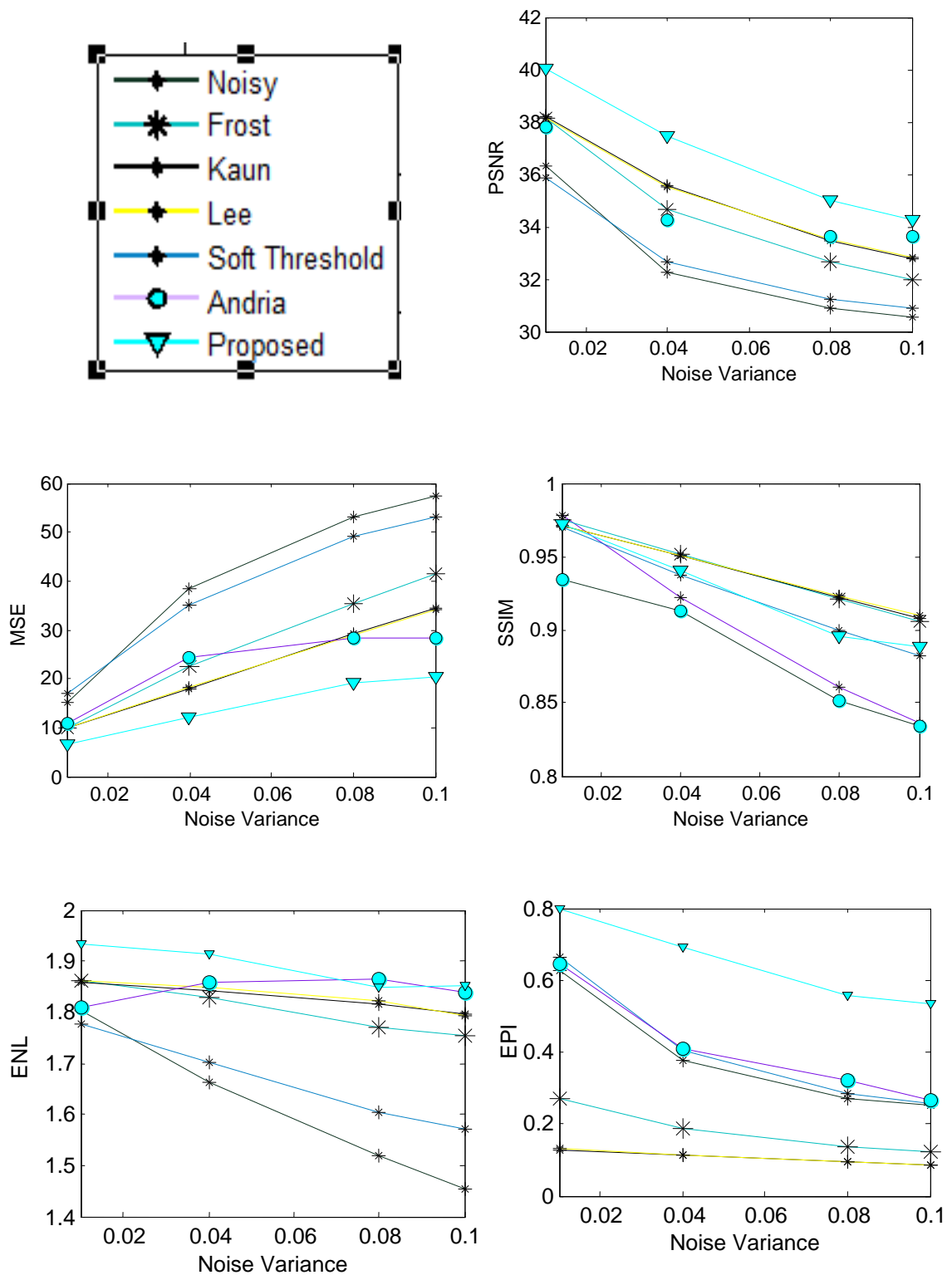


Figure 5.8 Graphical analysis of various performance measures of ISTWF for US image2

From Table 5.1 it is observed that the noise reduction ability is appreciably improved in ISTWF compared to Andria's approach. The values of SSIM, ENL and EPI show better improvement in high variances than Andria et al (2013). Therefore, the resulting image retains the important image features better than Andria et al (2013) and other filters. The visual quality enhancement of ISTWF is compared in relation to different noise variances for US image1 in Figure 5.7. The output images are enhanced with noise reduced and with good edge preservation.

The performance of ISTWF is tested with another clinical US image2 shown in Figure 3.7 and it is shown graphically in Figure 5.8. ISTWF is compared with standard speckle filters like Frost, Kuan and Lee filters, Soft thresholding approach and Andria et al (2013). The performance of ISTWF is better than the filters considered in all respects. For ENL the performances of ISTWF and Andria are equal.

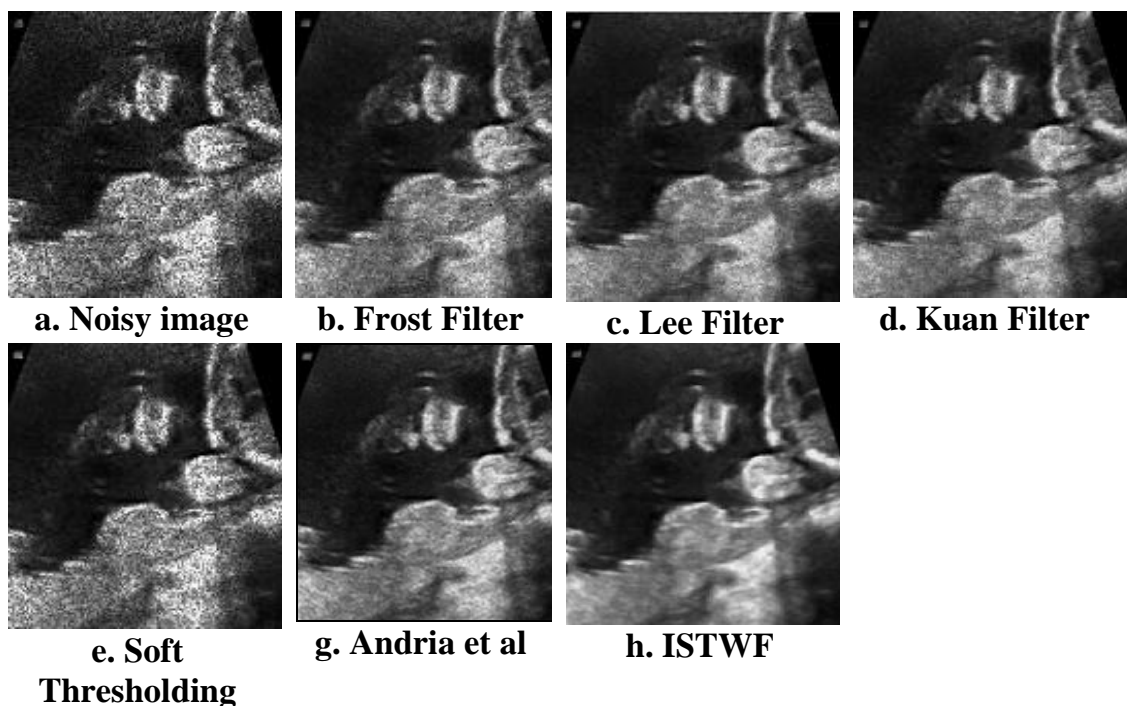


Figure 5.9 Comparison of visual quality of ISTWF with existing filters for US image3

Figure 5.9 shows the visual quality output of the various filters tested with sample US image 3 shown in Figure 3.8 for noise variance 0.1. It is clear from Figure 5.9 that the visual quality of ISTWF in Figure 5.9(h) is superior to the other filters considered. It shows improvement both in terms of noise removal and in important feature preservation. Hence it is clear that ISTWF provides better enhancement for the US images compared to the existing approaches. It is evident from the increased EPI values that the coefficients with low magnitude are reconstructed effectively. The result is achieved through the new exponential thresholding function defined in Equation (5.6). The proposed thresholding function gradually reduced the low magnitude coefficients around the threshold zone to zero using the exponential operator. The comparison of thresholding functions in Figure 5.3 shows that ISTWF achieves this better than soft computing and Andria et al (2013) approaches. And hence the low magnitude reconstructed coefficients approximate their original value rather than crowded near zero.

5.4 SUMMARY

This chapter discussed an inter scale adaptive threshold based speckle removal filter. It is designed to modify the low magnitude coefficients below the threshold. The proposed exponential thresholding function reduced the small magnitude coefficients gradually to zero by using an inter-scale adaptive threshold. It is determined using the inter-scale correlation or the parent-child relationship in the adjacent scale subbands. It identified more correctly the small magnitude significant coefficients at finer scales more appropriately than a single high threshold. Here the edge detection and edge evolution across scales is operated to scale the threshold according to their magnitudes, resulting in improved feature preservation. Also the proposed threshold is robust, in the sense that it adapts to the coefficient values according to the noise level and hence no empirical selection of parameters is required for



the selection of threshold. Hence, modification of the small magnitude coefficients using this threshold retained the fine image details thus improving the edge preservation index of the filter. The results and comparisons indicate that the proposed approach performs better than the existing filtering approaches in noise removal as well as in preserving edges and fine details.

